CHAPTER 5

MULTIVARIABLE NONLINEAR SYSTEM IDENTIFICATION

5.1 Introduction

In this chapter the results of nonlinear system identification are presented. Three different modeling approaches have been used. Neural network trained with Gradient Decent with Momentum (GDM) and Lavernberg Marquardt (LM) algorithm, Nonlinear State Space model and Adaptive Neuro Fuzzy Inference System (ANFIS). Modeling errors have been analyzed and discussed. Modeling approach has been done considering MISO system.

5.2 Neural Network Approach

5.2.1 Gradient Decent with Momentum (GDM)

For nonlinear system Identification the first approach which has been used is the Backpropagation Feedforward network trained using the delta rule (also known as gradient decent, with the addition of momentum). Modeling for both top and bottom temperature of the distillation column has been done with respect to the two inputs which are shown in Figure 3.5 for the reflux flow and Figure 3.6 for the steam flow of chapter 3. Figure 5.1 and 5.2 show the estimation result for top and bottom temperature of the distillation column. 2000 data points are used for estimation. Network architecture used is 2-10-1 and the model achieved its target within 57 epochs.

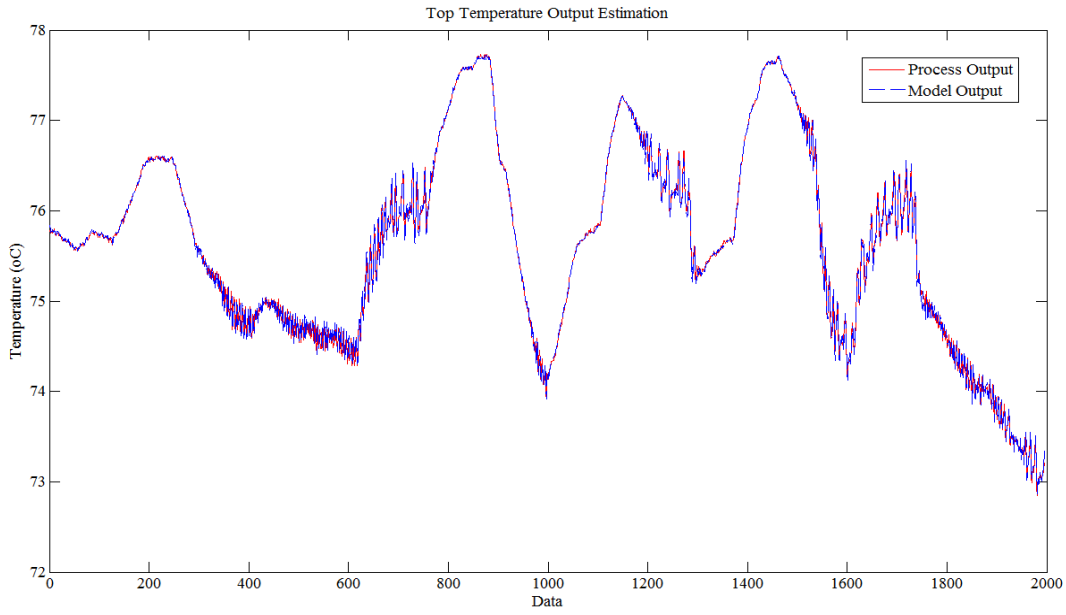

Figure 5.1: NN GDM Distillation Column Top Temperature Estimation.

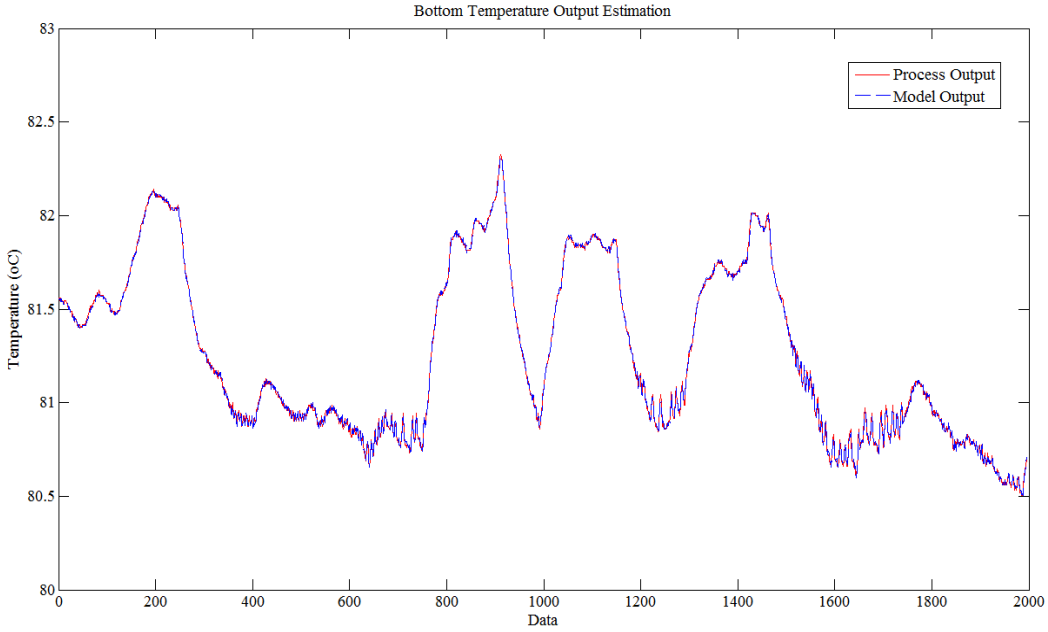

Figure 5.2: NN GDM Distillation Column Bottom Temperature Estimation.

Figure 5.3 and Figure 5.4 shows the validation result for top and bottom temperature of the distillation column. 2000 data points are used for Validation.

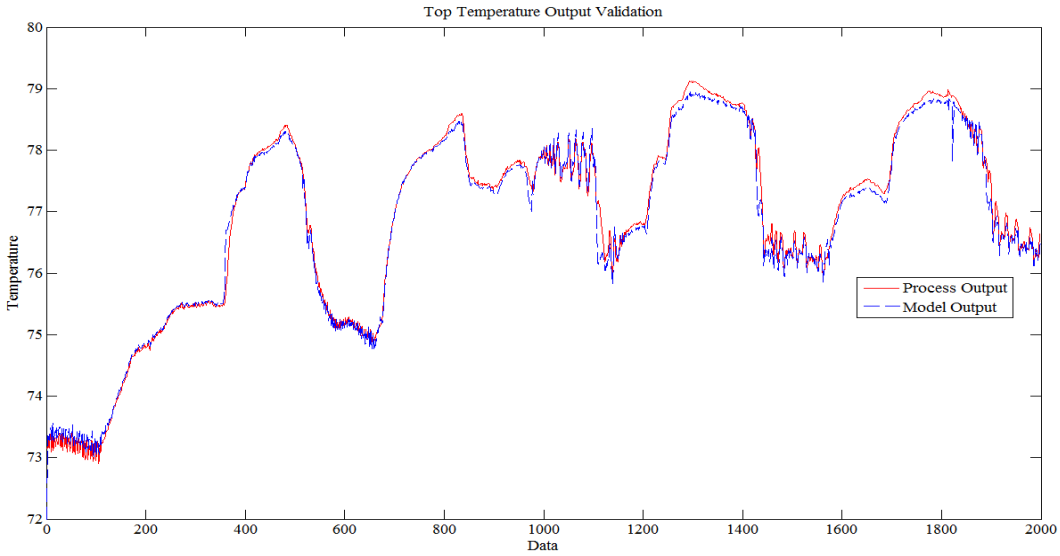

Figure 5.3: NN GDM Distillation Column Top Temperature Validation.

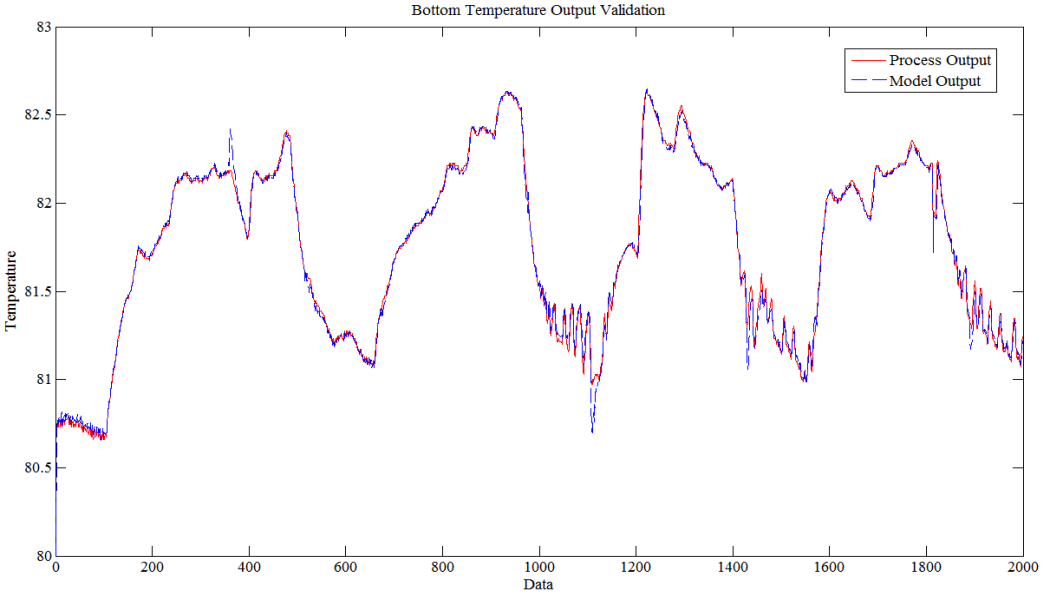

Figure 5.4: NN GDM Distillation Column Bottom Temperature Validation.

Identification of the APC plant by the NN trained by GDM algorithm shows a very significant result. The network is able to capture the dynamic changes of the process plant.

5.2.2 Lavernberg Marquardt (LM)

Lavernberg Marquardt algorithm for training a neural network is a very well known approach. Neural network trained with LM algorithm also is used for modeling the process plant. Modeling for both top and bottom temperature of the distillation column has been done with respect to the two inputs which are shown in Figure 3.5 for the reflux flow and Figure 3.6 for the steam flow of chapter 3. Figure 5.5 and 5.6 shows the estimation result for top and bottom temperature of the distillation column. 2000 data points are used for estimation. The models took 37 epochs to achieve its target with network architecture of 2-10-1.

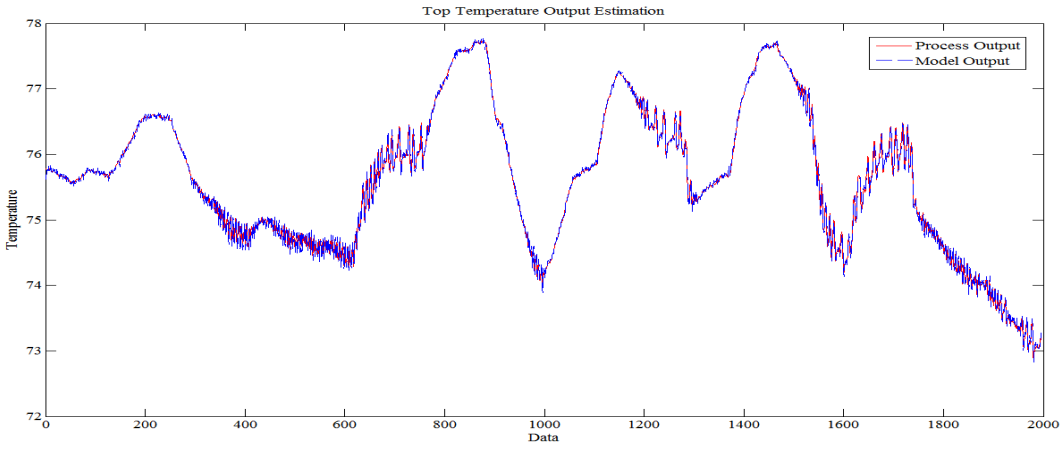

Figure 5.5: NN LM Distillation Column Top Temperature Estimation.

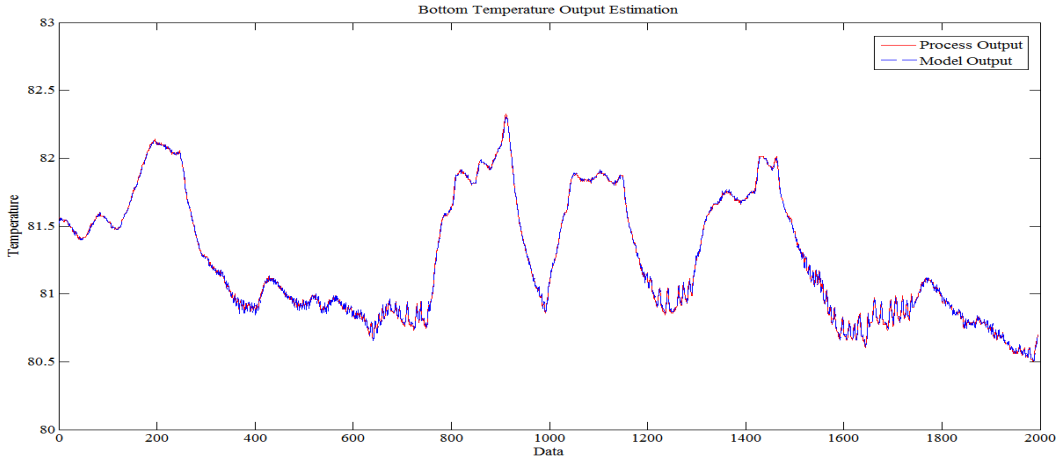

Figure 5.6: NN LM Distillation Column Top Temperature Estimation.

Figure 5.7 and Figure 5.8 shows the validation result for top and bottom temperature of the distillation column. 2000 data points are used for Validation.

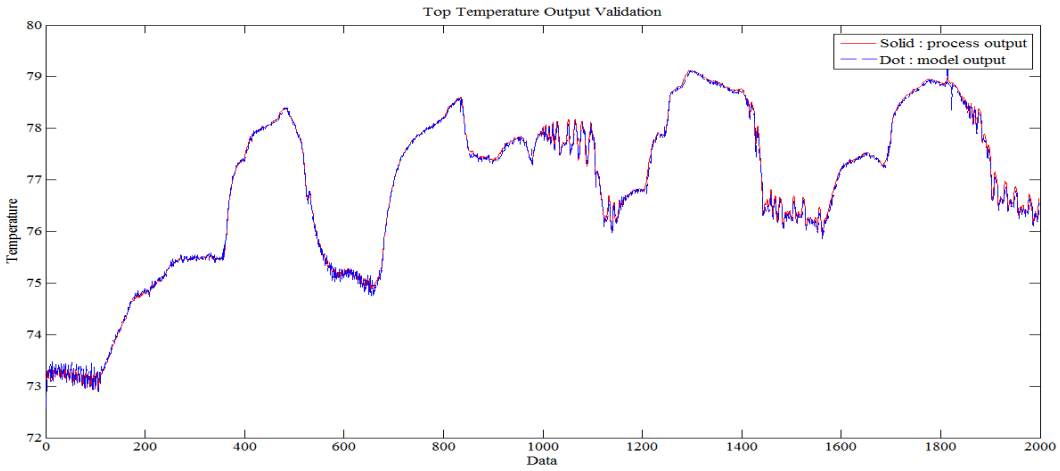

Figure 5.7: NN LM Distillation Column Top Temperature Validation.

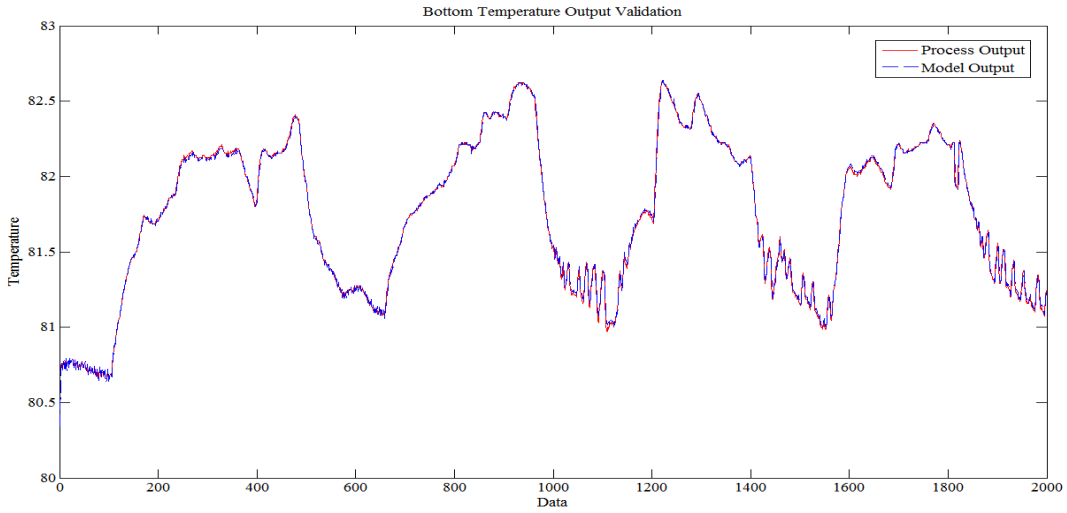

Figure 5.8: NN LM Distillation Column Bottom Temperature Validation.

Observing the resposne of the neural network trained with Laverberg Marqurdt algorithm, the nework is capable of capturing the changes in the dynamics of the nonlinear process.

5.3 Nonlinear State Space Model

A different type of approach using neural network, nonlinear state space model was developed in conjunction of linear state space model along with neural network as has been explained in Chapter 2. Modeling for both top and bottom temperature of the distillation column has been done with respect to the two inputs which are the reflux flow and the steam flow. The linear state space model of 3rd order discrete time system is used for developing the nonlinear state space model. The MISO forms of linear state space models obtained for top temperature of the system is given by equation 5.1 to 5.3. The equation is taken from the linear model discussed in chapter 4.

$$x(k+1)=\begin{bmatrix}0 & 0 & 0.4375\\ 1 & 0 & -1.3226\\ 0 & 1 & 1.881\end{bmatrix}x(k)+\begin{bmatrix}-0.04537 & -0.001\\ 0.6431 & 0.01\\ -0.646 & -0.00521\end{bmatrix}\begin{bmatrix}U_1 & U_2\end{bmatrix} \qquad (5.1)$$

The MISO linear state space model output equation obtained for top temperature of the system is given as;

$$y_1(k)=\begin{bmatrix}0 & 0 & 1\end{bmatrix}x(k)+\begin{bmatrix}0\end{bmatrix}\begin{bmatrix}U_1 & U_2\end{bmatrix} \qquad (5.2)$$

Where *x(k)* is the system state, $y_1(k)$ is the output of the system. The initial state *x(0)* of the system is given as;

$$x(0)=\begin{bmatrix}-0.00355\\ -0.017\\ -0.003\end{bmatrix} \qquad (5.3)$$

As stated in [24], when using neural network to identify the system two important assumptions are considered: (1) all the system states are measureable; (2) the system is stable. States for the physical system are considered to be measured and the stability of the system is observed by the pole-zero plots as shown in Figure 5.9 for top temperature process and Figure 5.10 for bottom temperature process. Observing

the graphs from Figure 5.9 and Figure 5.10, all the poles positions appears to be within the unity circle which shows the stability if the system.

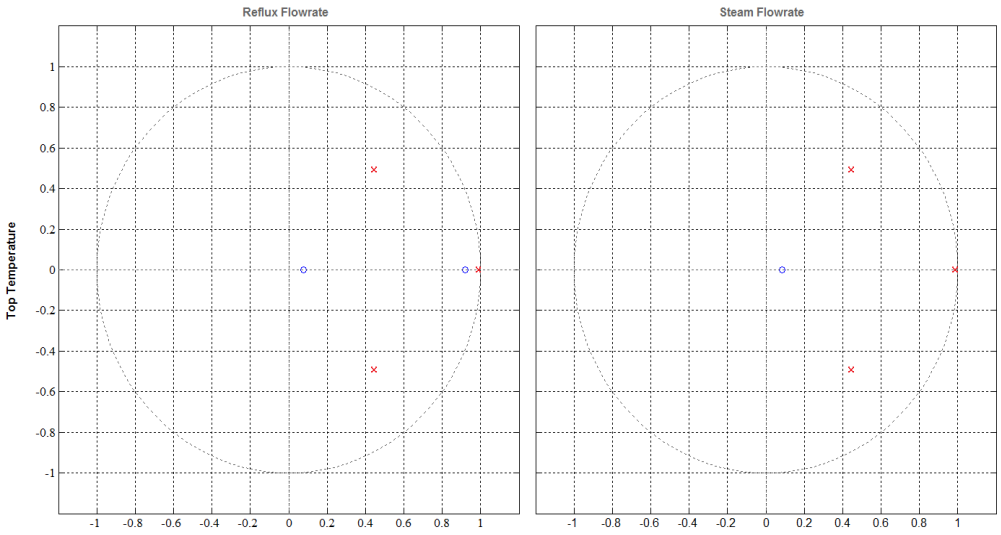

(a) (b)

Figure 5.9: (a) I/O Poles & Zeros from Input U_1 to Output Y_1
(b) I/O Poles & Zeros from Input U_2 to Output Y_1

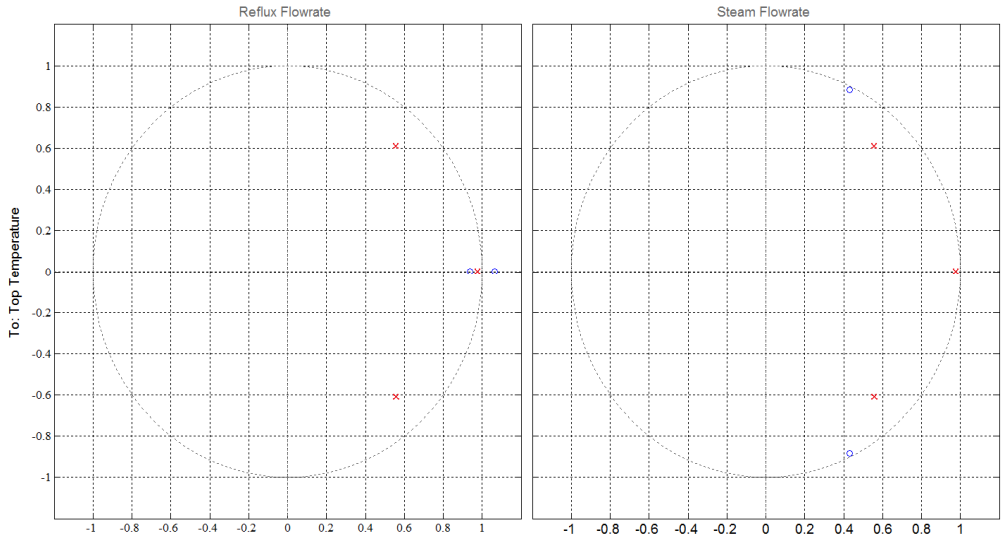

(a) (b)

Figure 5.10: (a) I/O Poles & Zeros from Input U_1 to Output Y_2
(b) I/O Poles & Zeros from Input U_2 to Output Y_2

Figure 5.11 and Figure 5.12 shows the estimation and validation result for top temperature of the distillation process column. 2000 data points are used for both estimation and validation.

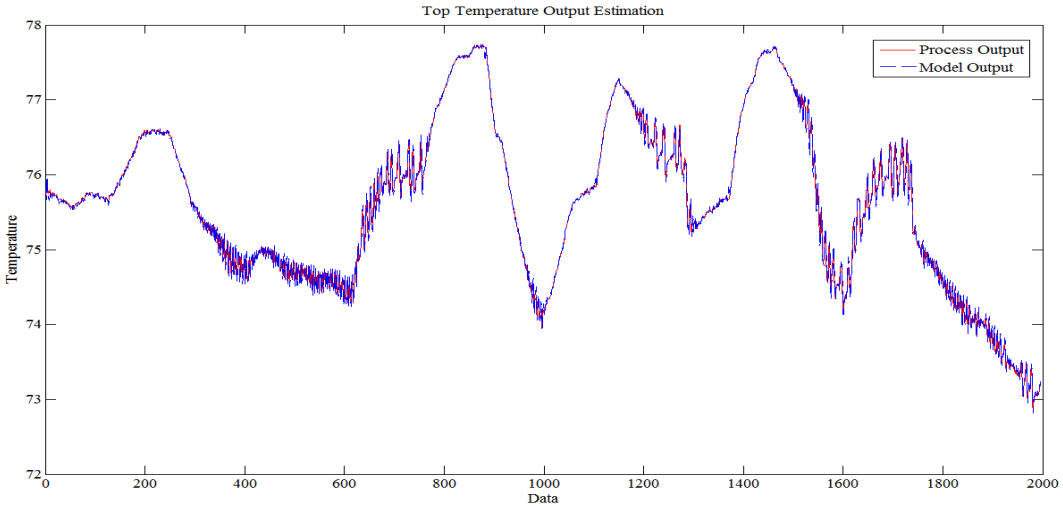

Figure 5.11: Nonlinear State Space Model for Top Temperature Estimation.

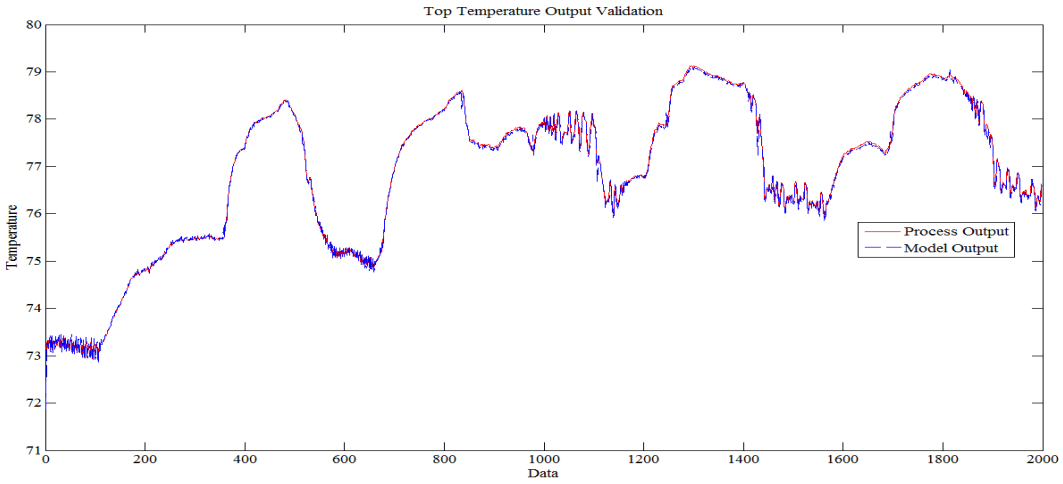

Figure 5.12: Nonlinear State Space Model for Top Temperature Validation.

The MISO forms of linear state space models obtained for bottom temperature of the system is given by equation 5.4 to 5.6. The equation is taken from the linear model discussed in chapter 4.

$$x(k+1)=\begin{bmatrix}0 & 0 & 0.67\\ 0.5 & 0 & -0.8872\\ 0 & 2 & 2.1\end{bmatrix}x(k)+\begin{bmatrix}-0.3861 & 0.00606\\ 0.4 & -0.002705\\ -0.4 & 0.0063\end{bmatrix}\begin{bmatrix}U_1 & U_2\end{bmatrix} \quad (5.4)$$

The MISO linear state space model output equation obtained for bottom temperature of the system is given as;

$$y_2(k)=\begin{bmatrix}0 & 0 & 0.5\end{bmatrix}x(k)+\begin{bmatrix}0\end{bmatrix}\begin{bmatrix}U_1 & U_2\end{bmatrix} \quad (5.5)$$

Where *x(k)* is the system state, $y_2(k)$ is the output of the system. The initial state *x(0)* of the system is given as;

$$x(0)=\begin{bmatrix}-0.013771\\ -0.004\\ -0.0033\end{bmatrix} \quad (5.6)$$

Figure 5.13 and Figure 5.14 shows the estimation and validation result for bottom temperature of the distillation column. 2000 data points are used for both estimation and validation.

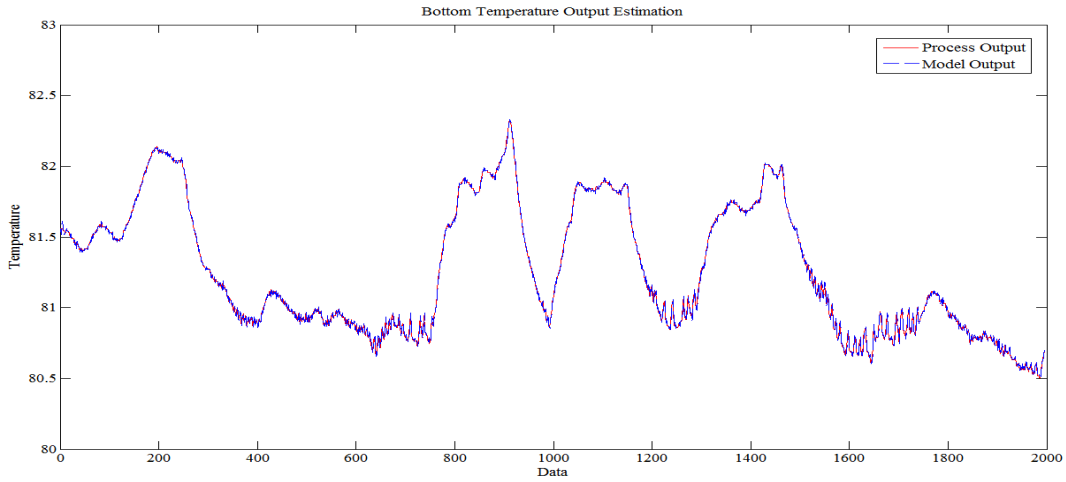

Figure 5.13: Nonlinear State Space Model for Bottom Temperature Estimation.

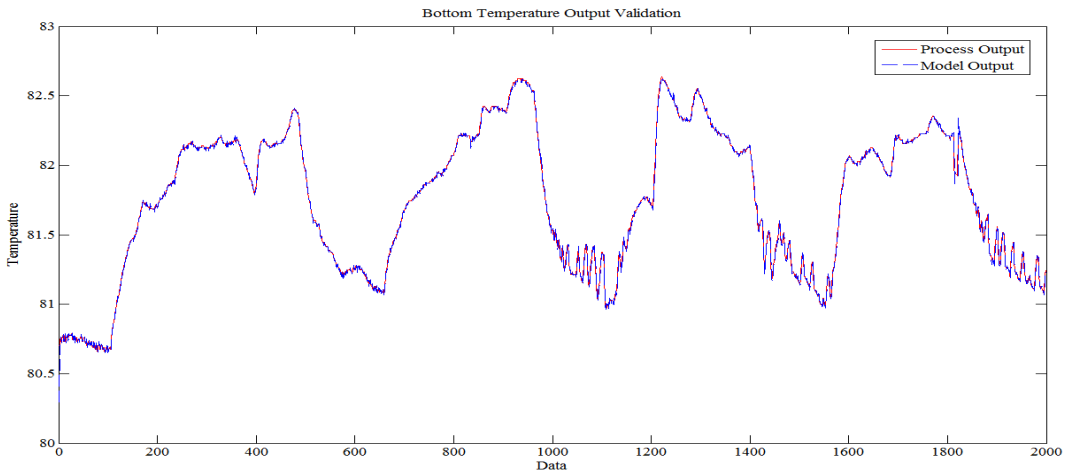

Figure 5.14: Nonlinear State Space Model for Bottom Temperature Validation.

Analysing the response of nonlinear state space model, the model is capable of capturing the nonlinear dynamic changes of the system. The error analysis for both top and bottom of the model are tabulated in Table 5.3 and Table 5.4.

5.4 Adaptive Neuro-Fuzzy Inference System

Adaptive Neuro Fuzzy Inference System is one another approach can be used for identifying nonlinear systems. In construction of ANFIS structure, parameters are determined. There are quite a few MFs such as Triangular, Trapezoidal and Gaussian can be used as an input MFs. Commonly used MFs in literature are the Triangular and Gaussian. For this reason, Sigmoid, Gaussian and Triangular are chosen as input MF type in this study. Number of MFs on each input can be chosen as 3, 5, and 7 to define the linguistic labels significantly.

Since, there is no typical method to employ the expert knowledge; automatic rule generation (grid partition) method is usually preferred [51]. According to this method, for instance, an ANFIS model with two inputs and three MFs on each input would result in 3^2=9 Takagi-Sugeno fuzzy if-then rules automatically. Although this method can require much computational knowledge especially in systems that have to be defined with many inputs, it is used in this study due to advantage of MATLAB

software. Therefore, rule bases of the estimators are formed automatically with the number of inputs and number of MFs. After the ANFIS structure is constructed, learning algorithm and training parameters are chosen. As mentioned in chapter 2, the hybrid learning algorithm is used in this study. Simulation has been performed for the top temperature and bottom temperature of the distillation column using ANFIS structure. Table 5.1 and Table 5.2 show the RMSE statistics of the ANFIS model.

Table 5.1: RMSE Estimation Performance Measurement for ANFIS structure

	Top Temperature			**Bottom Temperature**		
Membership Functions	3MFs	5MFs	7MFs	3MFs	5MFs	7MFs
Sigmoid	0.7578	0.7074	0.6781	0.2696	0.2597	0.2464
Gaussian	0.7490	0.6930	0.6770	0.2695	0.2569	0.2470
Triangular	0.7841	0.7111	0.7064	0.2774	0.2611	0.2501

Table 5.2: RMSE Validation Performance Measurement for ANFIS structure

	Top Temperature			**Bottom Temperature**		
Membership Functions	3MFs	5MFs	7MFs	3MFs	5MFs	7MFs
Sigmoid	1.0746	1.0107	1.0037	0.3115	0.304	0.2902
Gaussian	1.0834	1.0158	0.9943	0.3122	0.3028	0.2903
Triangular	1.1589	1.0451	0.9982	0.3299	0.3026	0.2918

Analyzing Table 5.2, 5 Gaussian type MF shows a good result with RMSE value of 1.0158 for top temperature and 0.3028 for bottom temperature. Although the other type MF shows similar result but due to higher number of rules, the computation for both learning and training phase could take a much longer time. Figure 5.15 and Figure 5.16 show the estimation and validation result of the ANFIS structure of the

Gaussian type with 5MFs modelled for top temperature of the distillation column. Membership functions and fuzzy inference rules are given in Appendix C.

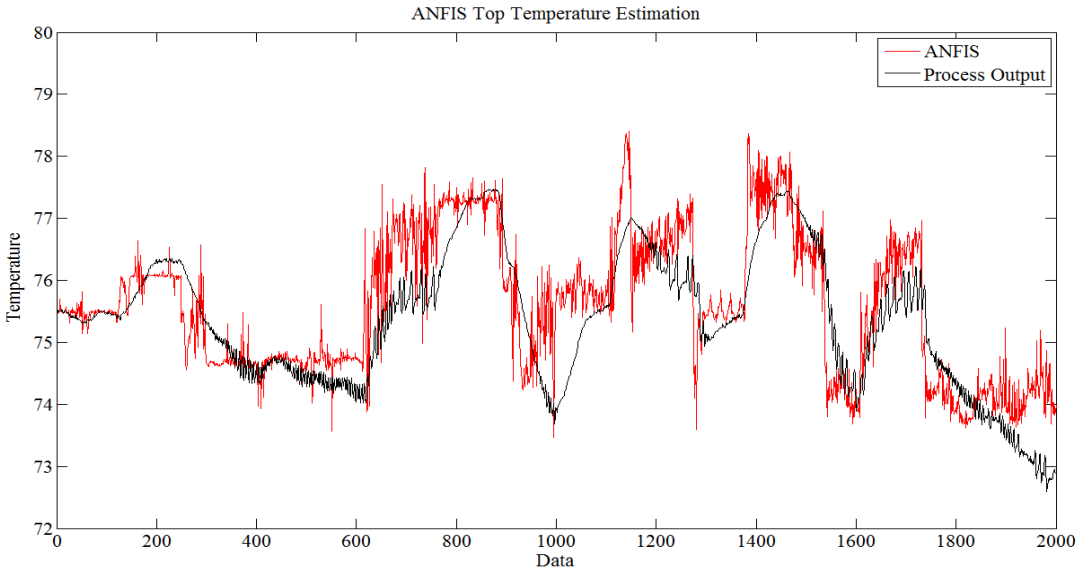

Figure 5.15: ANFIS Top Temperature Estimation.

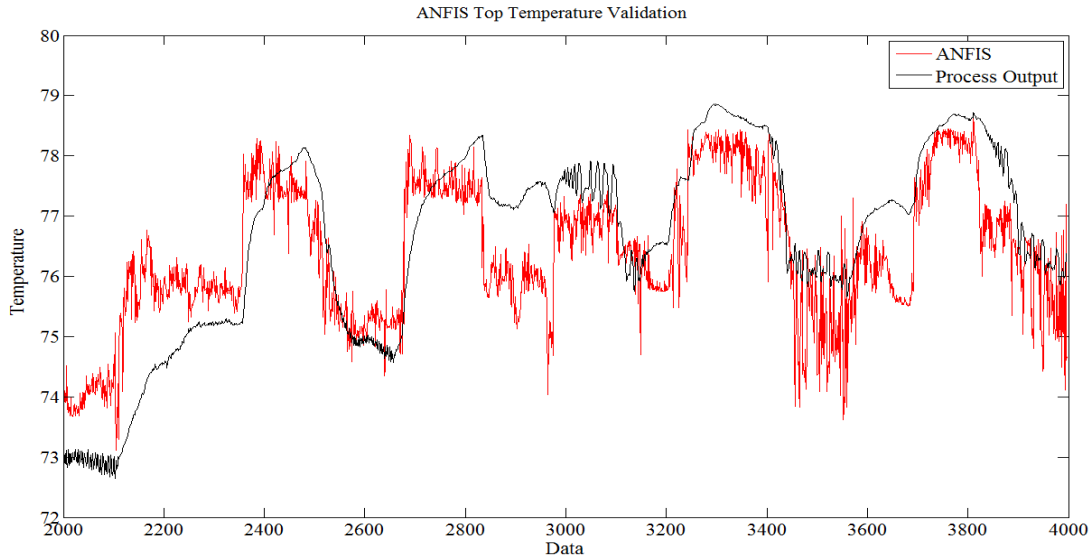

Figure 5.16: ANFIS Top Temperature Validation.

Analyzing Table 5.2, 5 Gaussian type MF shows a good result compared to other ANFIS approaches. Although 7 Gaussian and Triangular type MF shows similar result but due to higher number of rules, the computation for both learning and training phase could take a much longer time. The following Figure 5.17 and Figure

5.18 shows the estimation and validation result of the ANFIS structure of the Gaussian type with 5MFs modeled for bottom temperature of the distillation column. Membership functions and fuzzy inference rules are given in Appendix C.

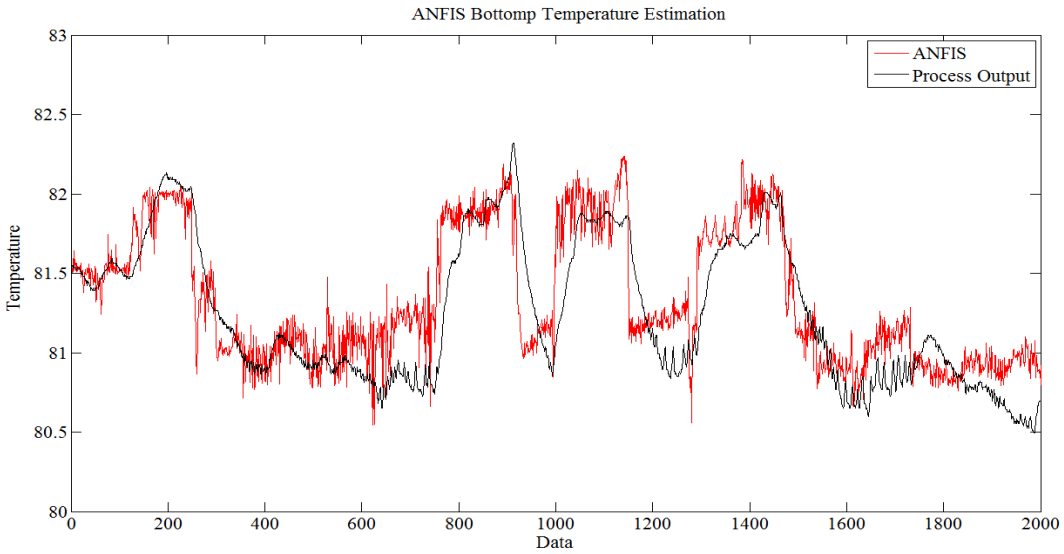

Figure 5.17: ANFIS Bottom Temperature Estimation.

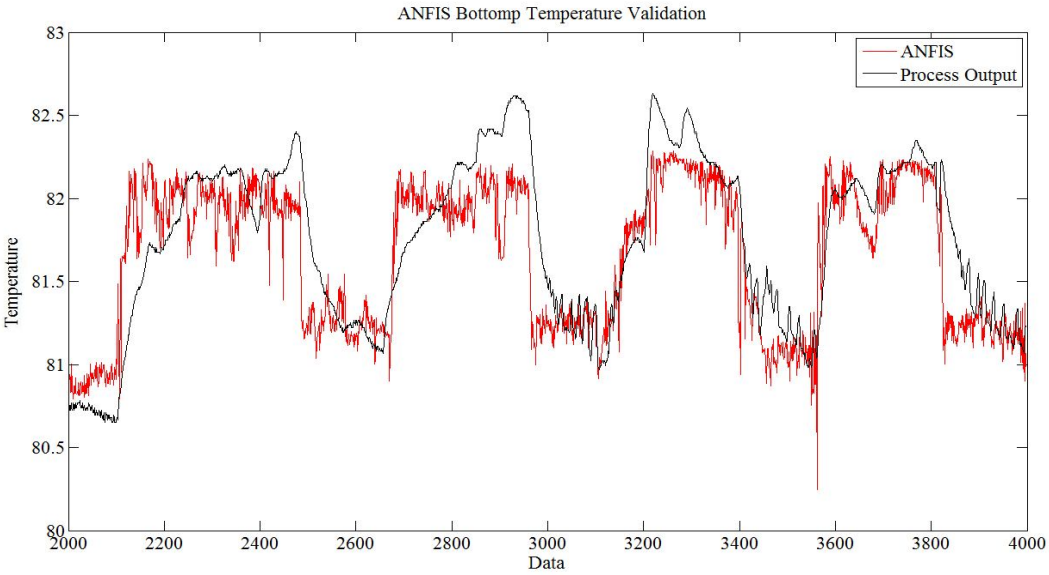

Figure 5.18: ANFIS Bottom Temperature Validation.

Looking into the ANFIS response both for top and bottom of temperature, the result is very noisy. This is because ANFIS is sensitive to noisy signals when given at the input. This is one reason that the ANFIS has not accurately modelled the input-output data's which in result shows that big error is present in the response.

5.5 Modelling Error Analysis

5.5.1 Best Fit Error Analysis

Following Table 5.3 shows the performance measurement of different types of nonlinear models.

Table 5.3: Numerical Results Performance Measurement for Top Temperature

Model Performance Measurement				
	Validation for Top		**Validation for Bottom**	
Model Structure	**Best Fit (%)**	**Sum of Squared Prediction Error**	**Best Fit (%)**	**Sum of Squared Prediction Error**
Gradient Decent Momentum	97.43	0.0120	98.44	0.0216
Lavernberg Marquardt	97.77	0.0312	98.39	0.0134
Nonlinear State Space	97.96	0.0162	99.38	0.0090
ANFIS	50.16	0.0997	60.13	0.0852

Analyzing Table 5.3, it can be observed that all the nonlinear models are capable of modeling the dynamic nonlinear system. Neural network trained by gradient decent with momentum and LM shows a very good result. The NSS model is also capable of identifying the dynamic nonlinear system. NSS model shows the best result with the best fit of 97.96% and 0.0162 SSPE for top temperature and 99.38% of best fit and 0.009 SSPE for bottom temperature process. ANFIS identification did not show a better result; this is because that every data point of the plant has to be evaluated from every rule defined in the ANFIS structure. Due to this process the computation takes a longer period and the process output observed is also noisy.

5.5.2 Nonlinear Identification Model Residual Analysis

5.5.2.1 Gradient Decent with Momentum

Figure 5.19 and Figure 5.20 show the predicted error or residual plot of the developed neural network model using GDM as the learning algorithm along with the residual histogram. These plots are based on the validation result of the model.

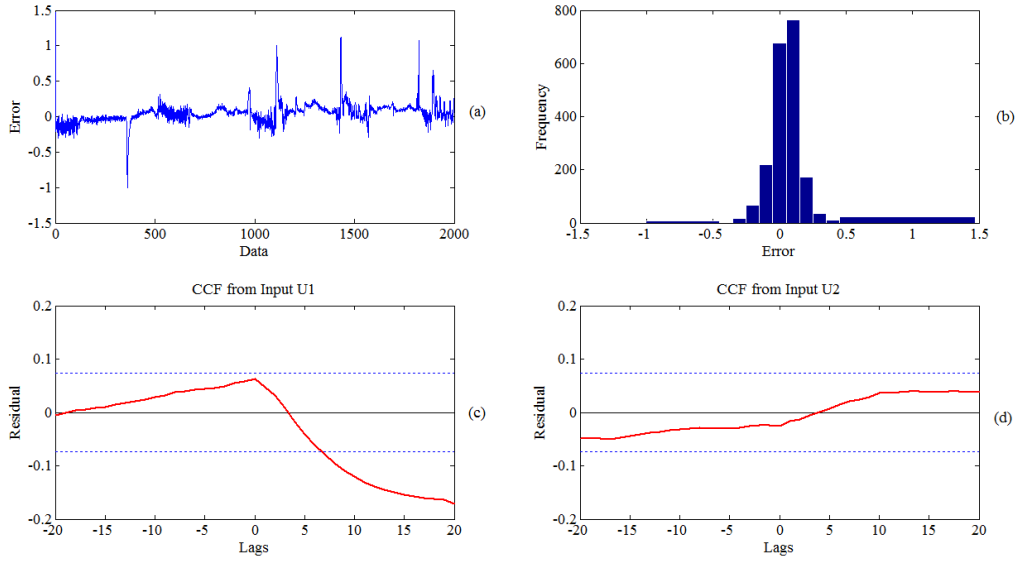

Figure 5.19: Residual Histogram for Top Temperature.

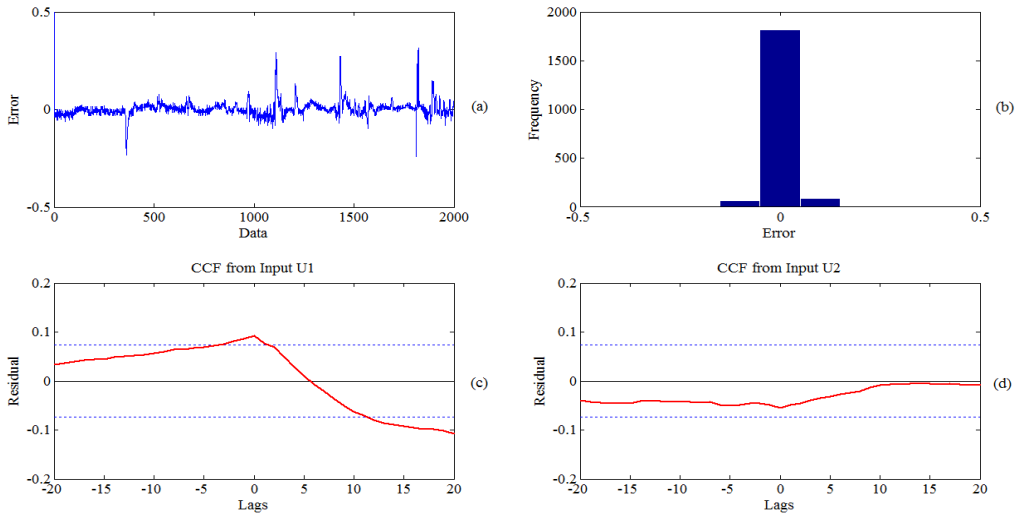

Figure 5.20: Residual Histogram for Bottom Temperature.

Observing Figure 5.19, the model does not show a proper histogram distribution for the validation data. Moreover, the cross-correlation graphs also show that the estimation data used for the development of the model did not completely modelled the top temperature of the process plant since correlation exits between the inputs and the residual. Observing Figure 5.20, the model validation shows a well distribution plot but the cross-correlation of the response shows that the estimation data used did not completely modelled the process plant as the graph has some values out of the 95% confidence interval boundary.

5.5.2.2 Lavernberg Marquardt

Figure 5.21 and Figure 5.22 show the predicted error or residual plot of the developed neural network model using LM as the learning algorithm along with the residual histogram. These plots are based on the validation result of the model.

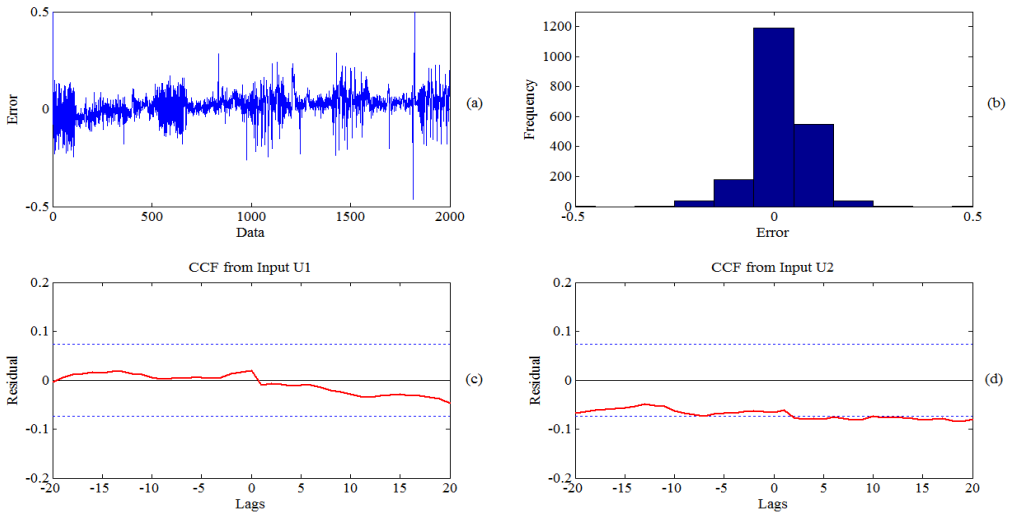

Figure 5.21: Residual Histogram for Top Temperature.

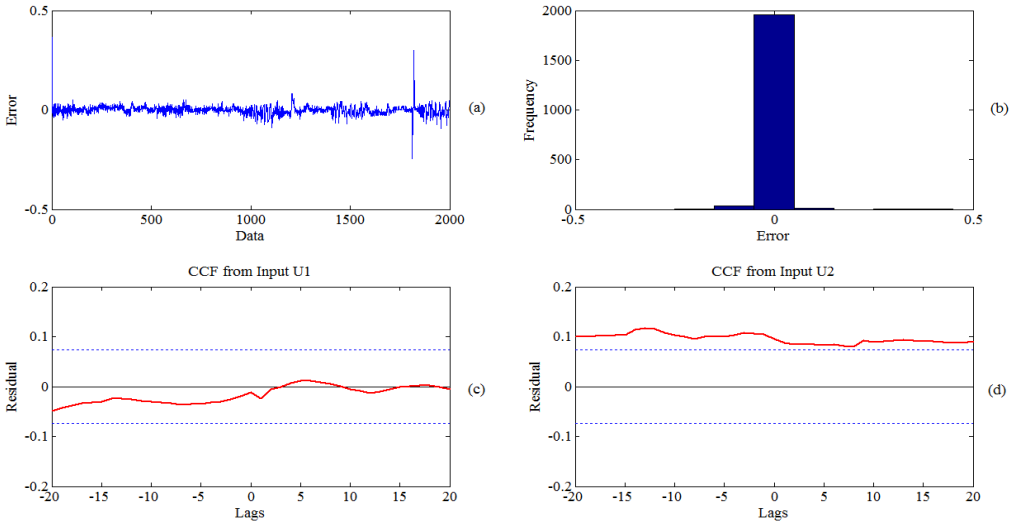

Figure 5.22: Residual Histogram for Bottom Temperature

Observing Figure 5.21, the model shows a proper histogram distribution for the validation data. Moreover, the cross-correlation graphs show that the estimation data used for the development of the model did not completely modelled the top temperature of the process plant since correlation exist between inputs and the residual. Observing Figure 5.22, the model validation shows a well distribution plot of the histogram but the cross-correlation of the response shows that the estimation data

used did not completely modelled the process plant as the graph has some values out of the confidence interval line.

5.5.2.3 Nonlinear State Space Model

Figure 5.23 and Figure 5.24 show the predicted error or residual plot of the developed NSS model along with the residual histogram. These plots are based on the validation result of the model.

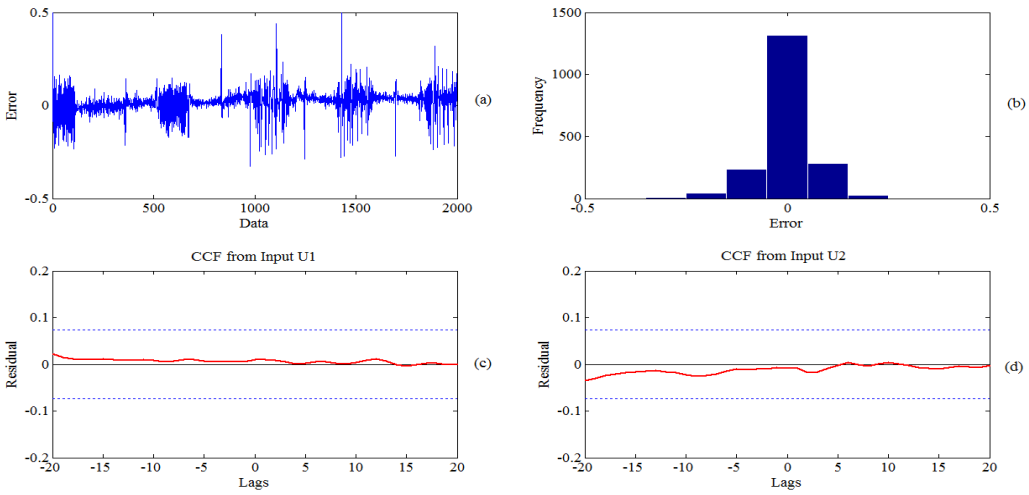

Figure 5.23: Residual Histogram for Top Temperature.

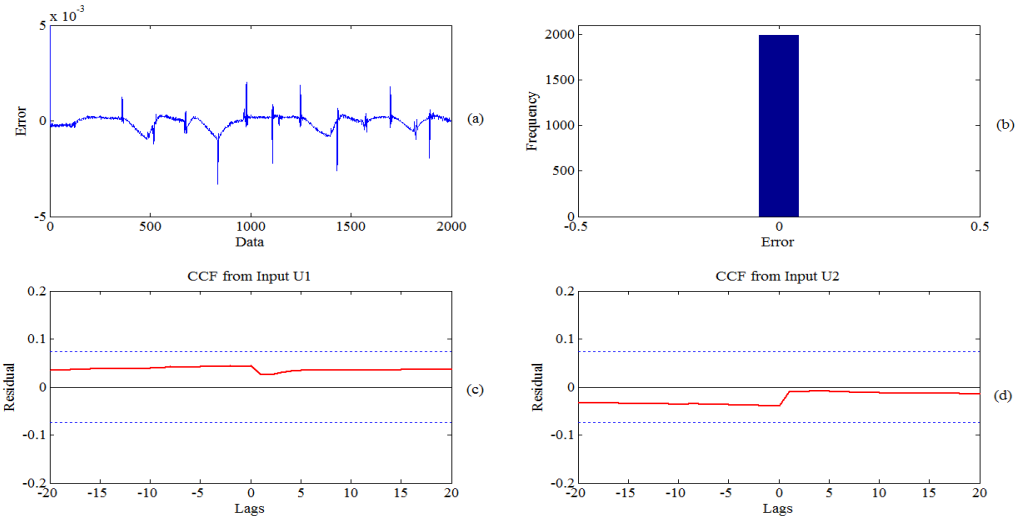

Figure 5.24: Residual Histogram for Bottom Temperature

Observing Figure 5.23, the model shows a well histogram distribution plot for the validation data. Moreover, the cross-correlation graphs also show that the estimation data used for the development of the model completely modelled the top temperature of the process plant since no correlation exist between the inputs and the residual. Observing Figure 5.24, the model validation shows a well distribution plot and also the cross-correlation of the response shows that the estimation data used completely modelled the process plant as the graph lies within the 95% confidence interval boundary.

5.5.2.4 ANFIS Model

Figure 5.25 and Figure 5.26 show the predicted error or residual plot of the developed ANFIS model using along with the residual histogram. These plots are based on the validation result of the model.

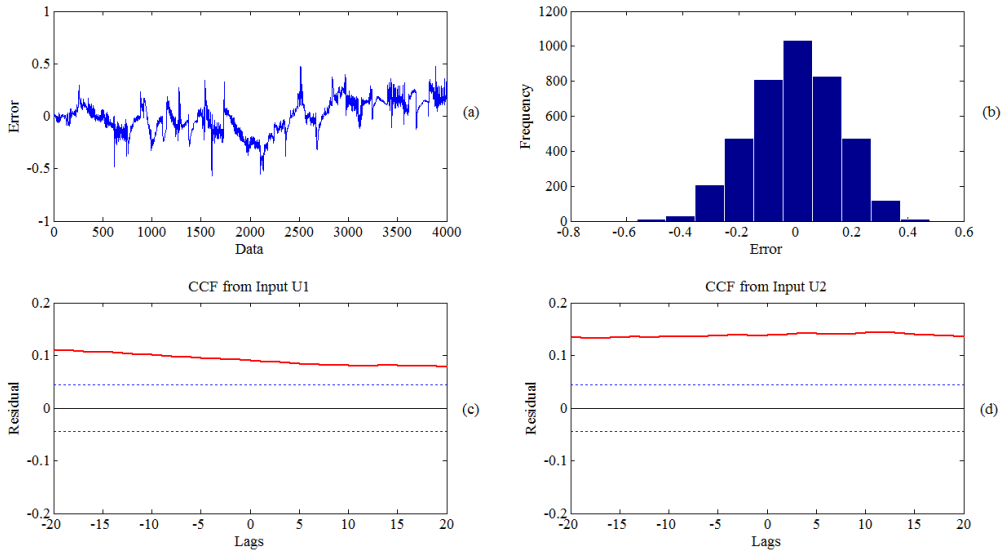

Figure 5.25: Residual Histogram for Top Temperature.

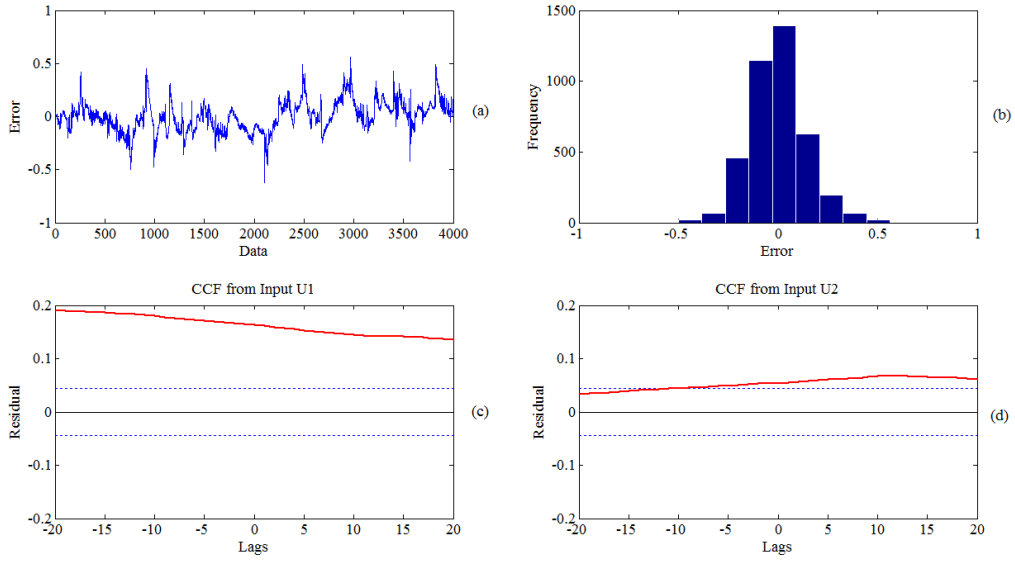

Figure 5.26: Residual Histogram for Bottom Temperature.

The ANFIS model shows a well distributed histogram response for both top and bottom temperature model of the process plant but the cross-correlation performance from input U_1 and input U_2 did not performed well since correlation exist with the residual.

Table 5.5 shows the mean and variance of the prediction errors for all the nonlinear models.

Table 5.4: Nonlinear Models Residual Histogram Performance Measurement

Model	**Top Temperature**		**Bottom Temperature**	
	Mean	**Variance**	**Mean**	**Variance**
GDM	0.0408	0.0020	0.0003	0.0002
LM	0.0021	0.0001	-1.917e-004	5.126e-004
NSS	2.3e-005	5.3e-005	4.61e-005	2.01e-005
ANFIS	0.8540	0.8670	0.2210	0.1850

Analysing the residual statistic of the developed nonlinear models from Table 5.5, it shows that Nonlinear State Space model shows a well compatible result to the

process output with the minimum mean value of 2.3e-5 and variance of 5.3e-5 for top temperature process and minimum mean 0f 4.61e-5 and 2.01e-5 for bottom temperature process. Neural network models also show a good compatible result. Analysing the residual histogram of these models, the graph is well distributed and centred at the origin. For ANFIS model, the residual is not well distribution at the centre for both top and bottom temperature models.

5.6 Summary

In this chapter, results has been shown and evaluated for different types of nonlinear models. The NN trained by GDM algorithm and LM, NSS model which is the combination of LSS models and NN trained by LM algorithm. All these models show a very significant result compared to the ANFIS. The simulation results shows that the identifier performance for estimating the model output is acceptable to some extend since the models are able to capture the changes in the dynamics of the process. Analyses of the result are given in Table 5.1, Table 5.2 and Table 5.3 and the best model results are highlighted. Further Analysis was performed by observing the prediction error and the residual histogram. Cross correlation testing is also observed from the two inputs U_1 and U_2. NSS model shows the best performance compared to all the other nonlinear models.